

<sup>20</sup>S. Chandrasekhar, *Rev. Mod. Phys.* **15**, 1 (1943); see also **15**, 61 (1943).

<sup>21</sup>Th. Förster, *Ann. Physik* **2**, 55 (1948); *Z. Naturforschg.* **4a**, 321 (1949).

<sup>22</sup>D. L. Dexter, *J. Chem. Phys.* **21**, 836 (1953).

<sup>23</sup>K. B. Eisenthal and S. Siegel, *J. Chem. Phys.* **41**, 652 (1964). It should be noted that for substitutional impurity molecules all dipoles may have the same orientation in which case  $\Phi$  will be closer to 0.84 than 0.67. This slight difference will have no effect on the subsequent discussion.

<sup>24</sup>M. Yokota and O. Tanimoto, *J. Phys. Soc. Japan* **22**, 779 (1967).

<sup>25</sup>C. E. Swenberg and W. T. Stacy, *Phys. Status Solidi* **36**, 717 (1969).

<sup>26</sup>Y. A. Kurskii and A. S. Selivanenko, *Opt. i Spektroskopiya* **8**, 643 (1960) [Opt. i Spectry. (USSR) **8**, 340 (1960)].

<sup>27</sup>R. Voltz, G. Laustriat, and A. Coche, *J. Chem. Phys.* **63**, 1253 (1966).

<sup>28</sup>R. Voltz, J. Klein, F. Heisel, H. Lami, G. Laus- strait, and A. Coche, *J. Chem. Phys.* **63**, 1259 (1966).

<sup>29</sup>K. H. Jones, *Mol. Cryst. J.* **3**, 393 (1968).

<sup>30</sup>W. L. Peticolas, J. P. Goldsborough, and K. E. Rieckhoff, *Phys. Rev. Letters* **10**, 43 (1963).

<sup>31</sup>The electron beam machine and a variety of super-radiant light targets are commercially available from

Field Emission Corporation, McMinnville, Oregon. This system is described in a paper by J. L. Brewster, J. P. Barbour, F. J. Grundhauser, and F. M. Charbonnier presented at the Twentieth Annual Meeting of the Société de Chimie-Physique, Paris, May, 1969 (unpublished).

<sup>32</sup>N. D. Galanin and Z. A. Chizhikova, *Opt. i Spektroskopiya* **1**, 175 (1956).

<sup>33</sup>W. G. Perkins, *J. Chem. Phys.* **48**, 931 (1968).

<sup>34</sup>V. L. Zima, A. D. Kravchenko, and A. N. Faidysh, *Opt. i Spektroskopiya* **20**, 441 (1966) [Opt. Spectry. (USSR) **20**, 240 (1966)].

<sup>35</sup>A. Suna (private communication).

<sup>36</sup>J. S. Avery, *Proc. Phys. Soc. (London)* **88**, 1 (1966).

<sup>37</sup>N. D. Zhevandrov, *Proceedings of the P. N. Lebedev Physics Institute*, 1965, (Consultants Bureau, New York, 1965), Vol. 25, p. 1.

<sup>38</sup>V. M. Agranovich, *Opt. i Spektroskopiya* **9**, 113 (1960) [Opt. Spectry. (USSR) **9**, 59 (1960)].

<sup>39</sup>J. D. Dow, Ph. D. thesis, University of Rochester, 1967 (unpublished).

<sup>40</sup>J. B. Birks, *Phys. Rev.* **94**, 1567 (1954).

<sup>41</sup>Reabsorption in these systems has been investigated by numerous authors, e.g., V. M. Agranovich, *Akad. Nauk SSSR Fiz.* **23**, 44 (1959); A. N. Faidysh, *ibid.* **23**, 53 (1959).

## Phase Transitions in Perovskitelike Compounds of the Rare Earths

S. Geller

Science Center, North American Rockwell Corporation, Thousand Oaks, California 91360

and

P. M. Raccah

Lincoln Laboratory, Massachusetts Institute of Technology, Lexington, Massachusetts  
(Received 16 March 1970)

High-temperature powder x-ray diffraction photography and differential thermal analysis give 1643 K for the rhombohedral-to-cubic transition temperature of  $\text{PrAlO}_3$ ; for  $\text{NdAlO}_3$ , this transition temperature is estimated to be 2020 K. The 800 K transition temperature of  $\text{LaAlO}_3$  is further confirmed. A rhombohedral-to-cubic transition temperature of 1230 K is predicted for  $\text{CeAlO}_3$ . The orthorhombic-to-rhombohedral transition temperatures of  $\text{LaFeO}_3$ ,  $\text{LaGaO}_3$ , and  $\text{SmAlO}_3$  have been corroborated; these are 1260, 1150, and 1075 K, respectively. Ruiz *et al.* have reported an orthorhombic-to-rhombohedral transition in  $\text{LaCrO}_3$  at 550 K, and the rhombohedral-to-cubic transition near 1300 K. The former occurs actually at  $533 \pm 3$  K, the latter above 1873 K and probably near 2000 K.

### INTRODUCTION

There has been substantial interest in the nature of the crystallographic transition in  $\text{LaAlO}_3$ .<sup>1</sup> A number of perovskitelike compounds of the rare-

earth ions are, in some temperature range, isostructural with  $\text{LaAlO}_3$ . Our purpose was to examine some of these and to determine their transition temperatures.

Two techniques were employed in two different

laboratories, but on the same specimens. The x-ray diffraction work and preparation of specimens were done at the Science Center; the differential thermal analyses (DTA) were performed at Lincoln Laboratory. In general, the results showed excellent agreement.

### EXPERIMENTAL

X-ray photographs were taken with a Bond high-temperature camera<sup>2</sup> built at the Science Center. Cu K $\alpha$  radiation was used for all photographs. Temperature calibration was carried out in three ways. (a) Originally a thermocouple was placed exactly in the specimen position and the furnace heated. The temperature given by this thermocouple was compared with that given by the thermocouple situated as shown in the Bond paper.<sup>2</sup> (b) The  $\alpha$ -versus- $T$  curve for yttrium iron garnet was determined<sup>3</sup> shortly after such a calibration. Then the YIG was used as a calibrant. (c) Some fixed points associated with first-order transitions obtained by differential thermal analysis verified the calibration at these points. It is likely that the temperatures differ from those recorded by no more than 5 K.

With the tedium of the large number of photographs to measure, the lattice-constant determination was made mainly from the measurement of several high angle lines. For the most part these lattice constants were not obtained by least-squares fit, although in some cases the program of Mueller *et al.*<sup>4</sup> was used. The accuracy of individual determinations could easily be overstated. However, the internal consistency of the results enhances their reliability.

Differential thermal analyses were carried out with a Du Pont 900 differential thermal analyzer.

The materials studied were all prepared<sup>5</sup> very carefully by reaction of appropriate amounts of high-purity rare-earth and transition-metal oxides. In some cases several regrindings and refirings were required to obtain sharply defined single phase materials. This is especially true of the specimen La<sub>0.65</sub>Pr<sub>0.35</sub>AlO<sub>3</sub>.

### RESULTS AND DISCUSSION

The lattice constants of the various compounds at various temperatures are listed in Table I. The lattice constants of the primitive rhombohedral cell are given in the second and third columns, those of the corresponding triply primitive cell are given in the fourth and fifth columns, while the volume per formula unit is given in the sixth column. Table II lists the results for some mixed rare-earth aluminates and also includes the volumes per formula unit predicted from the pure end members; for these it was assumed that

TABLE I. Crystallographic data for rhombohedral and cubic perovskitelike compounds.

$T(K)$	$a(\text{\AA})$	$\alpha-60^\circ(')$	Primitive cell		Hexagonal cell	
			$a(\text{\AA})$	$c(\text{\AA})$	$Vol(\text{\AA}^3)/(formula unit)$	$c(\text{\AA})$
(a) LaAlO <sub>3</sub>						
296	5.356	5.9	5.364	13.109	54.45	
473	5.363	4.5	5.369	13.129	54.63	
573	5.370	3.3	5.374	13.147	54.80	
673	5.375	2.0	5.378	13.164	54.96	
723	5.379	1.2	5.381	13.175	55.06	
798	3.807 <sup>a</sup>				55.18	
923	3.813 <sup>a</sup>				55.44	
1073	3.820 <sup>a</sup>				55.74	
1323	3.833 <sup>a</sup>				56.31	
(b) PrAlO <sub>3</sub>						
296	5.306	18	5.331	12.968	53.19	
523	5.321	15	5.340	13.010	53.54	
773	5.336	12	5.352	13.051	53.95	
973	5.352	9	5.364	13.094	54.38	
1173	5.365	8	5.376	13.130	54.77	
1400	5.381	5	5.387	13.173	55.18	
(c) NdAlO <sub>3</sub>						
296	5.288	23	5.319	12.916	52.74	
508	5.301	20	5.328	12.952	53.07	
708	5.313	16	5.334	12.988	53.34	
908	5.329	13	5.346	13.032	53.76	
1143	5.344	11	5.358	13.071	54.16	
1343	5.371	9	5.371	13.110	54.59	
(d) SmAlO <sub>3</sub>						
1073	5.309	18	5.333	12.976	53.27	
1373	5.333	14	5.352	13.041	53.92	
(e) LaCrO <sub>3</sub>						
533	5.474	41	5.530	13.338	58.88	
543	5.476	39	5.530	13.346	58.90	
873	5.496	32	5.540	13.408	59.39	
1173	5.519	23	5.551	13.479	59.95	
1373	5.533	18	5.558	13.521	60.29	
(f) LaFeO <sub>3</sub>						
1263	5.600	20	5.628	13.683	62.56	
1373	5.609	18	5.635	13.707	62.82	
(g) LaGaO <sub>3</sub>						
1153	5.538	20	5.567	13.531	60.53	
1373	5.558	16	5.580	13.589	61.07	

<sup>a</sup>Cubic.

the lattice constants are linear with mole fraction. The agreement of the predicted with the measured values is such as to indicate that the assumption is a sound one. If so, this implies a high probability that the crystallographic transition temperature is also linear with mole fraction of end member.

The first observation of the rhombohedral-to-cubic transition in LaAlO<sub>3</sub> was made by Geller

TABLE II. Lattice constants of mixed rare-earth aluminates.

T(K)	Primitive cell		Hexagonal cell Vol(Å <sup>3</sup> )/formula unit		
	a(Å)	α-60°(')	a(Å)	c(Å)	Measured-Predicted
<b>(a) (La<sub>0.65</sub>Pr<sub>0.35</sub>)AlO<sub>3</sub></b>					
296	5.338	11	5.353	13.057	54.01
473	5.346	10	5.360	13.077	54.23
673	5.363	6	5.371	13.126	54.65
873	5.375	4	5.381	13.159	54.99
973	5.382	3	5.386	13.174	55.16
1073	3.811 <sup>a</sup>				55.35
1123	3.913 <sup>b</sup>				55.44
1173	3.816 <sup>b</sup>				55.57
1273	3.821 <sup>b</sup>				55.79
1373	3.825 <sup>b</sup>				55.96
<b>(b) (La<sub>0.5</sub>Pr<sub>0.5</sub>)AlO<sub>3</sub></b>					
873	5.368	6	5.376	13.138	54.81
973	5.375	5	5.382	13.158	55.01
1073	5.382	3	5.386	13.179	55.19
1173	3.812 <sup>a</sup>				55.39
1233	3.815 <sup>b</sup>				55.52
1273	3.817 <sup>b</sup>				55.61
1373	3.821 <sup>b</sup>				55.79
<b>(c) (La<sub>0.65</sub>Nd<sub>0.35</sub>)AlO<sub>3</sub></b>					
973	5.375	4	5.381	13.159	55.00
1073	5.383	3	5.387	13.180	55.21
1123	5.387	2	5.390	13.192	55.32
1173	3.812 <sup>a</sup>				55.39
1223	3.815 <sup>b</sup>				55.52
1273	3.817 <sup>b</sup>				55.61
1373	3.821 <sup>b</sup>				55.79

<sup>a</sup>Probably not cubic.<sup>b</sup>Cubic.

and Bala,<sup>6</sup> who also reported that from the evidence it seemed "quite reasonable to conclude

that the transition from the rhombohedral to the cubic is of higher than first order." (It should be kept in mind that there is always some doubt, perhaps very small, that a transition is higher than first order, i.e., for example, the latent heat could be too small to measure.) The transition temperature reported by Geller and Bala,<sup>6</sup> however, was too low. Subsequent reports by others have shown it to be  $795 \pm 3$  K,<sup>7</sup> which is further corroborated by the present results. The volume/(formula unit) versus temperature (Fig. 1) has two linear portions with a break at 800 K.

Some earlier high-temperature results<sup>8</sup> on PrAlO<sub>3</sub>, SmAlO<sub>3</sub> and LaGaO<sub>3</sub> should be replaced by those given in the present report; the temperatures reported in the earlier measurements were generally low. Nevertheless, they all indicated that if the rhombohedral-to-cubic transition occurred in these at all, it would do so at very high temperatures.

In the more recent work, powder photographs of PrAlO<sub>3</sub> were taken to 1400 K at which temperature, as expected from the earlier measurements,<sup>7</sup> it is still rhombohedral (see Table I). Long extrapolations of hexagonal  $c/a$  to  $\sqrt{6}$ , or  $\alpha_{rh}$  to 60.00° could give incorrect results for the transition temperatures. Thus, a specimen (La<sub>0.65</sub>Pr<sub>0.35</sub>)AlO<sub>3</sub> was prepared and powder photographs taken at various high temperatures (Table II). As in the case of LaAlO<sub>3</sub>, a plot of volume versus temperature gave two straight line portions with a break<sup>9</sup> at 1110 K (Fig. 1). The back reflection lines of the x-ray powder photograph taken at 1073 K were broader than those taken at 1123 K and above. DTA gave  $1108 \pm 3$  K for the transition temperature. If the assumption of linearity is

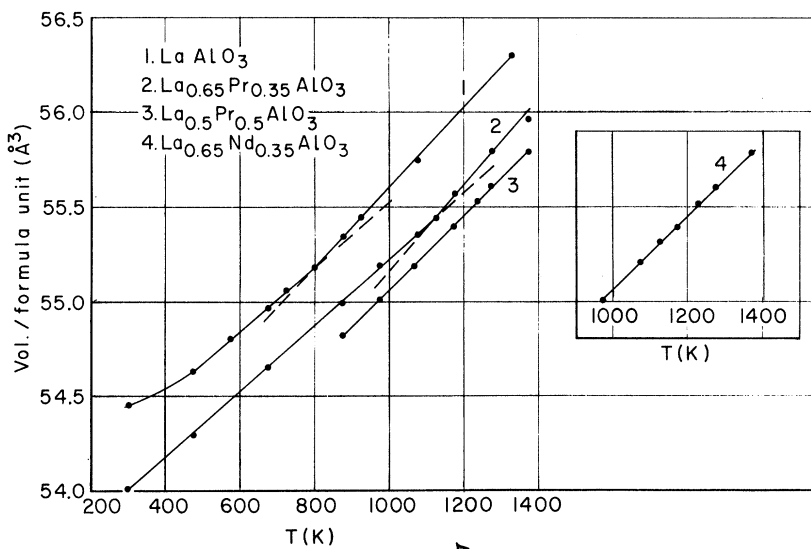


FIG. 1. Volume per formula unit versus temperature.

made, and 795 K is used as the transition temperature of  $\text{LaAlO}_3$ , one obtains 1690 K for the transition temperature of  $\text{PrAlO}_3$ . A differential thermal analysis of the  $\text{PrAlO}_3$  gave  $1643 \pm 5$  K for the transition.

For  $(\text{La}_{0.5}\text{Pr}_{0.5})\text{AlO}_3$ , no break was seen<sup>9</sup> in the plot of volume/(formula unit) versus temperature (Fig. 1). In this case, the x-ray powder photographs indicated that the transition occurred at 1233 K (or slightly lower). DTA gives  $1223 \pm 5$  K for this transition. Assuming linearity of transition temperature with composition, 1670 and 1650 K are obtained for the transition temperature of  $\text{PrAlO}_3$ . This approach appears to give the transition temperature to within 50 K. See Fig. 2 for a plot of transition temperature  $T_t$  versus composition.

Not presently understood is the observation from the DTA of  $\text{PrAlO}_3$  that its specific heat appears to undergo a slow modification of behavior over the range 973–1173 K. This may be indicative of a variation in one of the high-order derivatives of the free energy. There is no obvious change of structure in the x-ray powder photographs, and a possible nonlinearity in the thermal expansion in this range is not discernible by the technique used here.

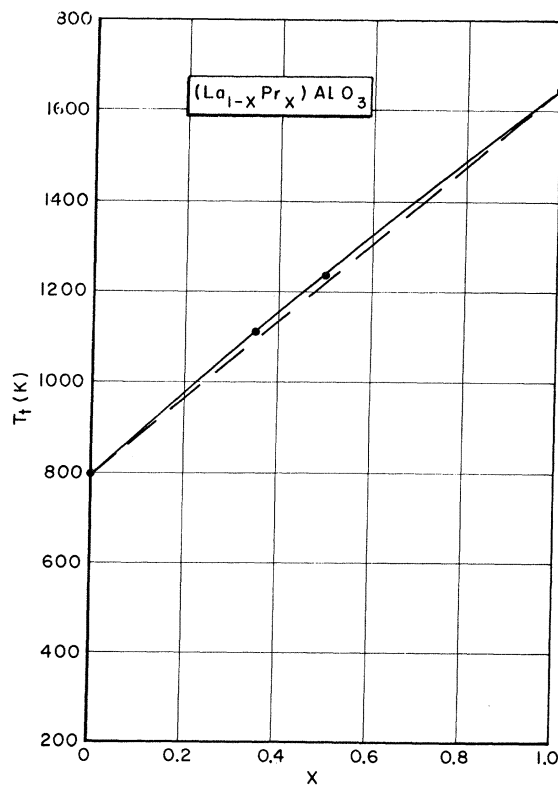


FIG. 2. Transition temperature versus composition.

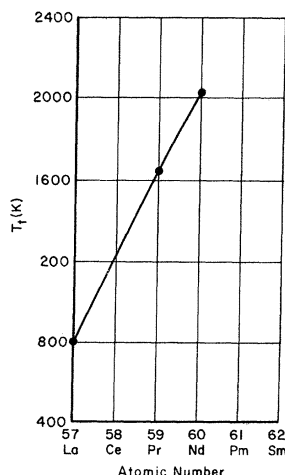


FIG. 3. Transition temperature versus atomic number.

For  $(\text{La}_{0.65}\text{Nd}_{0.35})\text{AlO}_3$ , the plot (Fig. 1) of volume/(formula unit) versus temperature again did not show a break, but the powder photographs indicated that the transition temperature was very near 1223 K and was estimated to be 1233 K. DTA gives  $1225 \pm 5$  K for this transition. Again, assuming linearity of transition temperature versus composition, the predicted transition temperature of  $\text{NdAlO}_3$  is 2050 and 2023 K, respectively. (DTA indicates that the transition of  $\text{NdAlO}_3$  itself occurs above 1873 K.)

If a smooth line is drawn through the three values of transition temperature, 795, 1643, 2020 K for the La, Pr,<sup>10</sup> and Nd<sup>10</sup> aluminates, respectively, plotted versus atomic number (Fig. 3), a transition temperature of 1230 K is predicted for  $\text{CeAlO}_3$ .

$\text{LaCrO}_3$  is orthorhombic and isostructural with  $\text{GdFeO}_3$  at room temperature.<sup>8</sup> Two transitions in  $\text{LaCrO}_3$  have been reported by Ruiz *et al.*<sup>11</sup> Their transition temperatures, however, appear to be incorrect. The first transition is from orthorhombic to rhombohedral, which we have found to occur between 528 and 533 K by x-ray powder diffraction photography and  $533 \pm 3$  K by DTA as opposed to 550 K reported by Ruiz *et al.* We also obtain a slightly higher value for the length of the hexagonal  $a$  axis than they reported at this temperature. Pavlikov *et al.*<sup>12</sup> have found this transition of  $\text{LaCrO}_3$  to occur at 560 K by differential thermal analysis, but they are not clear on the crystallography.

Ruiz *et al.*<sup>11</sup> have also reported that when the temperature of the rhombohedral phase is increased, "cette structure évolue progressivement et tendrait à devenir cubique type perovskite au-dessus de 1300 °K ( $a = 3.92 \text{ \AA}$  à 1500 K)." The two transitions appeared on their resistivity-ver-

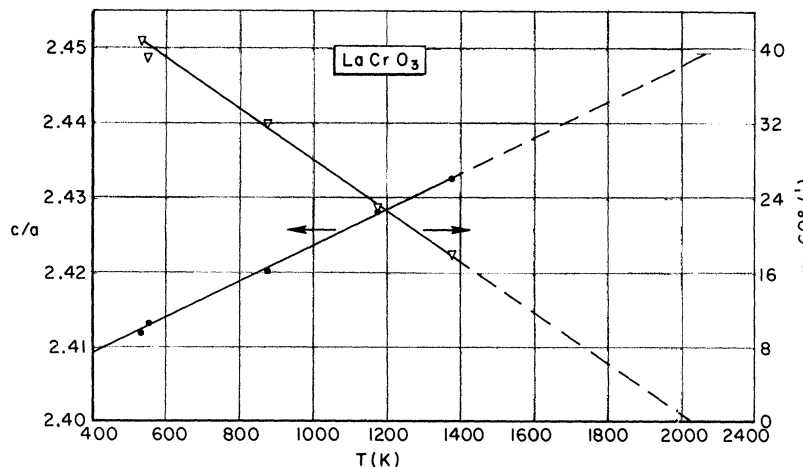


FIG. 4.  $c/a$  ratio and rhombohedral angle  $\alpha$ , less  $60^\circ$ , versus temperature.

sus-temperature curves. As well as can be determined from their figure, the graph for their specimen, which had been made by melting, shows breaks at 565, 630, 970, and 1450 K.

At 1373 K, there is no doubt that  $\text{LaCrO}_3$  is rhombohedral; the lattice constants are given in Table I. Further, it is very unlikely that  $\text{LaCrO}_3$  is cubic even at 1500 K. When the rhombohedral phase becomes cubic, the  $c/a$  ratio (in the hexagonal description) is equal to  $\sqrt{6}$ . A plot of  $c/a$  versus temperature is shown in Fig. 4. While it is not necessary that this plot be linear, it is highly unlikely that the behavior would be as required by a rhombohedral-to-cubic transition temperature of 1500 K. As indicated above, it is impossible that such a transition occurs in  $\text{LaCrO}_3$  near 1300 K.

There is still considerable distortion from the cubic at 1373 K; the rhombohedral angle is  $60^\circ 18'$ . Between 533 and 1373 K, the decrease of this angle is only  $23'$  (see Table I). Linear extrapolations of  $c/a$  versus temperature to  $c/a = \sqrt{6}$  and of angle  $\alpha$  to  $60^\circ$  predict a transition temperature of  $\sim 2000$  K. While it is possible (even probable) that the linear relation of both breaks down as the transition temperature is approached, there is little doubt that the transition in  $\text{LaCrO}_3$  occurs well above 1500 K. DTA confirms the absence of the rhombohedral-to-cubic

transition below 1873 K. The lattice constant at 1500 K reported by Ruiz *et al.* gives a volume per formula unit of  $60.2 \text{ \AA}^3$ ; this is less than the volume per formula unit of the rhombohedral  $\text{LaCrO}_3$  at 1373 K (Table I).

As an additional check, a specimen of  $\text{LaCrO}_3$  was prepared independently at Lincoln Laboratory. DTA gave the same results as for the Science Center specimen.

The results of DTA measurements on  $\text{SmAlO}_3$ ,  $\text{LaGaO}_3$ , and  $\text{LaFeO}_3$  were reported<sup>6, 8</sup> over a decade ago. These have first-order transitions at 1070, 1150, and 1250 K, respectively. For  $\text{SmAlO}_3$  and  $\text{LaGaO}_3$  these were found to be orthorhombic-to-rhombohedral transitions by high-temperature x ray diffraction powder photography.<sup>8</sup> New measurements have been made for this report.  $\text{LaFeO}_3$  also transforms to the rhombohedral phase. These results are consistent with a progression from orthorhombic to rhombohedral to cubic with increasing temperature.<sup>6, 8</sup> Lattice constants obtained at various temperatures above the transition temperature are given in Table I.

#### ACKNOWLEDGMENTS

All the powder photographs were taken by P. B. Crandall. Most of the specimens were prepared by G. P. Espinosa. C. H. Anderson assisted with the differential thermal analyses.

<sup>1</sup>For a review, see S. Geller, *Phys. Status Solidi* (to be published).

<sup>2</sup>W. L. Bond, *Rev. Sci. Instr.* **29**, 654 (1958).

<sup>3</sup>S. Geller, G. P. Espinosa, and P. B. Crandall, *J. Appl. Cryst.* **2**, 86 (1969).

<sup>4</sup>M. H. Mueller, L. Heaton, and K. T. Miller, *Acta Cryst.* **13**, 828 (1960). Revised by J. Gvildys in 1964.

<sup>5</sup>S. Geller, H. J. Williams, R. C. Sherwood, and G. P. Espinosa, *J. Phys. Chem. Solids* **23**, 1525 (1962).

<sup>6</sup>S. Geller and V. B. Bala, *Acta Cryst.* **9**, 1019 (1956).

<sup>7</sup>H. Fay and C. D. Brandle, in *Crystal Growth* (Pergamon, New York, 1967), p. 51; *J. Appl. Phys.* **38**, 3405 (1967); K. A. Müller, W. Berlinger, and F. Waldner, *Phys. Rev. Letters* **21**, 814 (1968).

<sup>8</sup>S. Geller, Acta Cryst. **10**, 243 (1957).

<sup>9</sup>As can be seen from Table II, this is predicted also by linear interpolation between values of lattice constants of the end members.

<sup>10</sup>The  $T_t$ 's predicted for  $\text{PrAlO}_3$  and  $\text{NdAlO}_3$  by J. F. Scott [Phys. Rev. **183**, 823 (1969)] are, respectively,

320 and 380 K too low.

<sup>11</sup>J. S. Ruiz, A. Anthony, and M. Foëx, Compt. Rend. **264**, 1271 (1967).

<sup>12</sup>V. N. Pavlikov, L. M. Lopato, and S. G. Tresvyat-skii, Izv. Akad. Nauk SSSR Neorgan. Materialy **2**, 679 (1966).

## Two-Phonon Resonances and Hybridization of the Resonance with Single-Phonon States\*

J. Ruvalds and A. Zawadowski<sup>†</sup>

Department of Physics, University of Virginia, Charlottesville, Virginia 22903

(Received 14 January 1970)

Considering the anharmonic phonon-phonon interactions, two-phonon resonances are studied by Green's-function methods. The two-phonon spectrum exhibits an asymmetric peak near the top of the two-phonon continuum. In the special case of a resonance consisting of two acoustic phonons, the hybridization of the resonance with a single optical phonon is possible, in agreement with experiment.

It has recently been proposed<sup>1</sup> that the anharmonic phonon-phonon interaction can give rise to two-phonon bound states which explain the anomalous peak observed in the second-order Raman spectrum of diamond.<sup>2,3</sup>

The purpose of the present work is to show that phonon-phonon interactions can have a striking influence on the *first-order* as well as the second-order spectrum. First we show that the second-order spectrum is modified in an essential way by the formation of two-phonon resonances under quite general conditions, in contrast to the case of two-phonon bound states which can occur only for a limited range of anharmonic coupling. Furthermore, we demonstrate that the first-order spectrum may exhibit structure as a result of hybridization of a two-phonon resonance with single-phonon states.

We wish to relate our results to Raman scattering experiments and therefore consider only resonances with total momentum  $\vec{K} = 0$ .<sup>4</sup> In the case of resonances consisting of optic-mode phonons the momenta of the individual phonons  $\vec{k}_1$  and  $\vec{k}_2$  obey the relation  $\vec{k}_1 = -\vec{k}_2 \approx 0$ . For resonances of acoustic phonons, the individual phonons have wave vectors  $\vec{k}_1 = -\vec{k}_2 = \vec{k}^i$ , where the  $\vec{k}^i$  ( $i = 1, 2, \dots$ ) refer to equivalent edges of the Brillouin zone. In both cases the resonance is formed from states near the top of the phonon band.

The Hamiltonian including third- and fourth-order anharmonic terms can be written as  $\mathcal{H}$

$= \mathcal{H}_{\text{harmonic}} + \mathcal{H}_3 + \mathcal{H}_4$ , where  $\mathcal{H}_{\text{harmonic}}$  is the usual phonon Hamiltonian in the harmonic approximation. The third-order term  $\mathcal{H}_3$  will contribute to the finite lifetime of the single-phonon excitations. We include these broadening effects for the single-phonon states by means of a phenomenological width  $\Gamma$ , which will be considered as a constant in the energy range of interest.

Since the phonon energies of interest are much greater than the thermal energies considered experimentally, we employ the Green's-function formalism for zero temperature. The effects of finite temperature can then be included in the phenomenological parameters which enter into the calculation.

Following the usual notation,<sup>5</sup> we introduce a propagator for a single phonon

$$D_1(\vec{k}, \omega) = \frac{1}{2} \omega(\vec{k}) \{ [\omega - [\omega(\vec{k}) - \frac{1}{2}i\Gamma]]^{-1} - [\omega + [\omega(\vec{k}) - \frac{1}{2}i\Gamma]]^{-1} \}, \quad (1)$$

where  $\omega(\vec{k})$  is the single-phonon energy and  $\Gamma$  is a phenomenological width against decay into other phonons, for example, the decay of a single optic phonon into two acoustic phonons. The above Green's function is the Fourier transform of the usual Green's function in the coordinate representation  $D_1(x, x') = -i \langle T[\phi(x)\phi(x')] \rangle$ , where  $T$  denotes the time-ordering operator and the phonon field amplitudes<sup>5</sup>  $\phi(x)$  are given by